JGR Space Physics

RESEARCH ARTICLE
10.1029/2020JA028713

Centrifugal Equator in Jupiter's Plasma Sheet

Phillip Phipps[1], **and Fran Bagenal**[2]

[1]University of Maryland, Baltimore County, Baltimore, MD, USA, [2]Laboratory for Atmospheric & Space Physics, University of Colorado, Boulder, CO, USA

Key Points:

- Between 5 and 30 jovian radii, the equatorial current sheet increasingly changes the magnetic field geometry from a dipole to a disk
- The centrifugal equator correspondingly changes from 2/3 to the full magnetic dipole tilt
- We derive a simple formulation for the centrifugal equator versus distance and System III longitude

Correspondence to:
F. Bagenal,
bagenal@lasp.colorado.edu

Citation:
Phipps, P., & Bagenal, F. (2021). Centrifugal equator in Jupiter's plasma sheet. *Journal of Geophysical Research: Space Physics*, *126*, e2020JA028713. https://doi.org/10.1029/2020JA028713

Received 22 SEP 2020
Accepted 16 DEC 2020

Abstract In Jupiter's magnetosphere, the structure of the plasma sheet depends on the magnetic field geometry and the centrifugal forces on the plasma. We present a simple formulation for the centrifugal equator, the farthest point along a magnetic flux tube from the planetary spin axis, for Jupiter's torus to plasma sheet region (5–30 jovian radii). The formulation is based on a dipole magnetic field and azimuthally symmetric current sheet, both tilted by 9.5° toward System III west longitude of 201°. We find a good fit to such a model with a hyperbolic tangent function varying sinusoidally with longitude. The latitudinal angle of the derived centrifugal equator relative to the jovigraphic equator changes from the dipolar value (2/3 of the dipole tilt) around 5 jovian radii to close to the full dipole tilt at 25 jovian radii.

1. Introduction

The goal of this study is to address how large-scale magnetic field geometry controls the structure of Jupiter's plasma sheet. Gledhill (1967) was the first paper to appreciate the importance of the centrifugal potential in confining thermal plasma in Jupiter's fast-rotating magnetosphere and showed the Gaussian vertical distribution of an equatorial disk. Hill et al. (1974) derived the centrifugal equator, the farthest point along a magnetic flux tube, for a dipole field to be 2/3 the tilt angle, θ_m, of the magnetic equator from the planetary spin equator. Hill and Michel (1976) and Siscoe (1977) extended the discussion to consider how the thickness of the plasma disk would vary with ion species and temperature as well as distance from Jupiter for potential sources at the different Galilean satellites. This simple scale height distribution about a tilted centrifugal equator was subsequently applied to both remote sensing of emissions as well as in situ plasma measurements in the Io plasma torus (see review by Thomas et al., 2004). Ambipolar diffusion of a multispecies plasma, including effects of thermal anisotropy and supra-thermal (e.g., kappa) populations, have been applied to Voyager, Ulysses, and Galileo data sets (e.g., Bagenal, 1994; Mei et al., 1995; Meyer-Vernet, 2001; Moncuquet et al., 2002). These studies focused on the Io plasma torus (~6–10 R_J, where the magnetic field is reasonably approximated by a tilted dipole and 1 R_J = 71,492 km is a Jupiter radius).

Inward of about 5 R_J, the nondipolar components of the magnetic field become increasingly significant. In the warm torus (>5.6 R_J), the effective vertical scale height of the plasma is ~1.2 R_J while in the cold torus (<5.4 R_J), the very low temperatures and small (<0.2 R_J) scale height mean the location of the centrifugal equator is sensitive to high-order structure of the magnetic field. For example, Bagenal (1994) found that extrapolation of in situ Voyager plasma data along the field was very sensitive to the magnetic field model. Herbert et al. (2008) analyzed high resolution optical images of S^+ emissions and reported a vertical offset from the (dipole) centrifugal equator with longitude that is probably due to nondipole components. The high-order structure of Jupiter's magnetic field derived from Juno's close flybys of the planet (Connerney et al., 2018) may eventually allow accurate modeling of such fine-scale features.

Beyond the torus region, where the plasma becomes spread out into a disk and the local currents distort the planetary magnetic field, the issue arises of where the centrifugal equator is located. Figure 1 shows the geometry of the magnetic field and the locations of the different equators in the meridional plane in jovicentric coordinates where the vertical direction is Jupiter's spin axis and the horizontal axis is the spin or rotational equator. The jovigraphic, magnetic and centrifugal equators are shown on the left for longitudes where the equators align and on the right for longitudes of maximum magnetic dipole tilt angle, θ_m. The centrifugal equator is shown at $\theta_c = 2/3\ \theta_m$, in accordance with the Hill et al. (1974) dipole formulation. As the influence of the current sheet increases from 5 to 30 R_J the farthest point from the spin axis moves toward the magnetic equator, so that θ_c becomes θ_m.

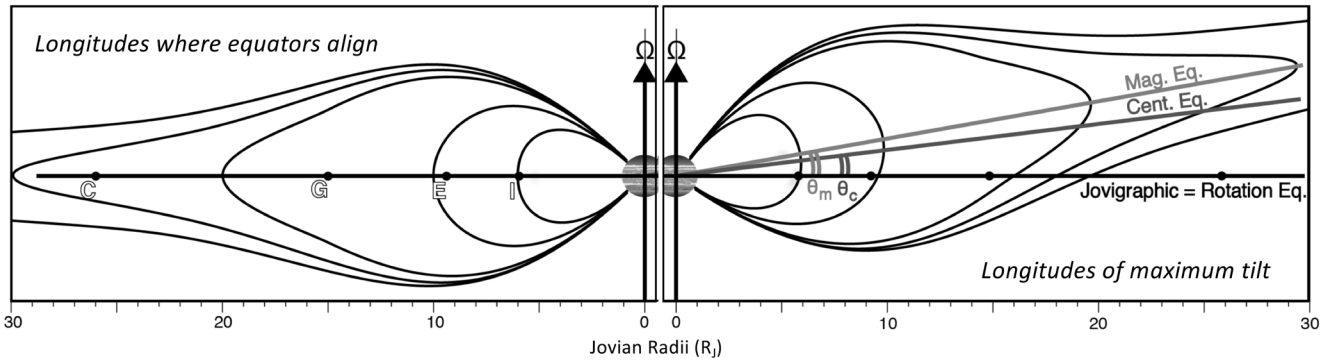

Figure 1. Geometry of jovigraphic, magnetic, and centrifugal equators for (left) longitudes where the equators align (Wlon = 111°, 291°, Elon = 249°, 69°) and (right) longitudes of maximum dipole tilt angle, θ_m, (Wlon = 21°, 201°, Elon = 339°, 159°). As the influence of the current sheet increases from 5 to 30 R_J, the tilt of the centrifugal equator (the farthest point from the spin axis along a magnetic fluxtube) increases from $\theta_c = 2/3\ \theta_m$ to $\theta_c = \theta_m$. The orbital distances of Io, Europa, Ganymede, and Callisto are shown.

2. Field Models

To facilitate analysis of the distribution of plasma, the 5–30 R_J region of the torus and plasma sheet we apply a simple dipole magnetic field and current sheet model. The problem is which dipole tilt angle and direction to use. Pre-Juno the Voyager-era magnetic field models such as Connerney et al. (1998)'s VIP4 have a dipole tilt of 9.5° toward System III longitude of Wlon = 201° in the traditional west or left-handed system (where an observer, say from Earth, sees Jupiter's subsolar longitude increase with time). In the east or right-handed system, this would be Elon = 360–201 = 159°. Other models that focus on phenomena close to the planet (e.g., aurora or radio emissions) incorporate higher-order structure and produce dipole approximations with slightly different tilts and directions (e.g., Hess et al., 2011). The recent magnetic field model based on Juno data obtained very close to Jupiter reveals considerable structure in the magnetic field (Connerney et al., 2018) which is crudely approximated by a dipole tilted at 10.31° toward Wlon = 196.61°. Since we are interested in the region > 5 R_J, we take the dipole that is derived from data in that region and apply the VIP4 value of 9.5° toward System III longitude of Wlon = 201°.

Current sheet models have also been developed with considerable complexity. Most notably, the Khurana model (Khurana, 1997; Khurana & Schwarzl, 2005) combines internal magnetic field components (e.g., VIP4), an equatorial current sheet that varies with local time, plus currents in the magnetotail and on the magnetopause. The parameters of the model have been derived by matching magnetic field data, primarily from Galileo. But for the inner region of the magnetosphere (<30 R_J) we can start with an azimuthally symmetric current sheet that is primarily just a simple washer-shaped volume (inner, outer radius R_0, R_1) with an azimuthal ("ring") current that is uniform over a fixed half-thickness (D), with a $1/\rho$ variation with distance, ρ, from Jupiter's dipole axis. This is the Voyager-based Connerney et al. (1981) model (sometimes called CAN81).

Connerney et al. (2020) have adapted CAN81 to match the first 24 orbits (July 2016–December 2019) of data from Juno to produce a model that varies with time. The azimuthal current varies about 6% between orbits while the radial current is about 10 times smaller but more variable (~40% level). Connerney et al. (2020) find that the average current sheet in the Juno-era is slightly thicker (D = 3.6 R_J) and weaker ($\mu_0 I/2$ = 140.2 nT) than the Voyager-era current sheet of CAN81 (D = 2.5 R_J, $\mu_0 I/2$ = 185 nT).

3. Centrifugal Equator Derivation

To derive farthest point from spin axis, the centrifugal equator, in the 5–30 R_J region, we use a dipole equivalent appropriate for this region (i.e., VIP4 of 9.5° toward System III longitude of Wlon = 201°) and a current disk similar to Connerney et al. (2020) with D = 3.6 R_J, $\mu_0 I/2$ = 140.2 nT, R_0 = 7.8 R_J, R_1 = 50 R_J which we tilt to the same 9.5° toward Wlon = 201°. We call this current sheet model CON2020.

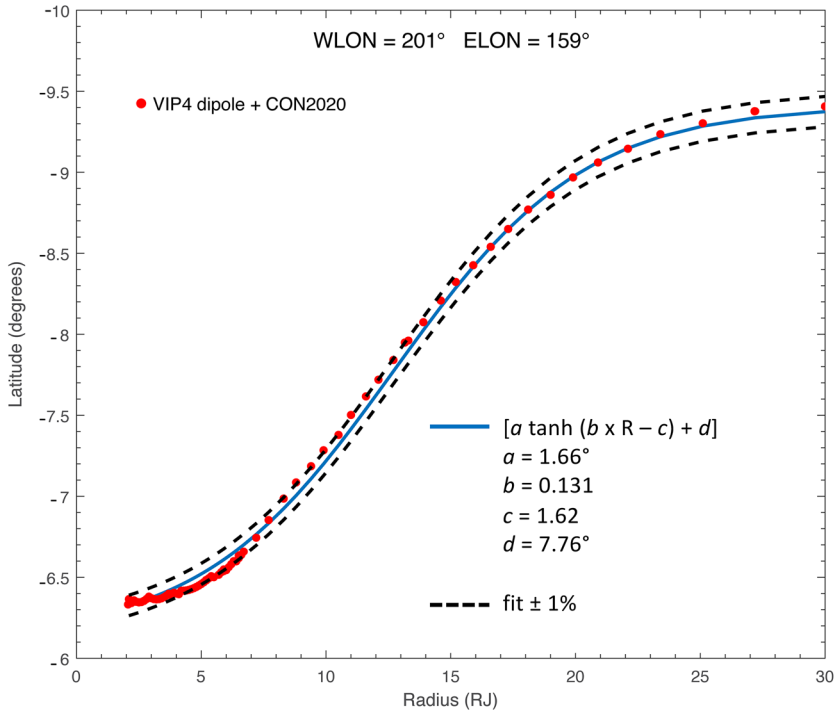

Figure 2. Jovigraphic latitude of the centrifugal equator at Wlon = 201°, Elon = 159° for the VIP4dipole + CON2020 model (dots) with fit to hyperbolic tangent function (line).

Mapping field lines using this VIP4dipole + CON2020 model from pole to pole we then find the farthest point from Jupiter's spin axis for different longitudes. The mapping starts at the jovigraphic equator (at a co-latitude of 90 degrees) at each radial distance and longitude. We then follow the field line until the field line reaches the Jovian surface (defined as an oblate spheroid). Figure 2 shows the model locations (red dots) of the centrifugal equator for Wlon = 201°, Elon = 159°. These points were then fit with a hyperbolic tangent function (blue line) which matches the VIP4dipole + CON2020 model quite well. The resulting latitude of the centrifugal equator from the jovigraphic equator (in degrees) is given by this function

$$\mathrm{CentEq2}\left(R\right) = a\tan h\left(b\times \mathrm{R} - c\right) + d \tag{1}$$

where R is the jovigraphic radial distance (in R_J) and the values of the parameters a, b, c, and d are given in Table 1. The model points were matched by this simple curve to within ~1% accuracy. The model points in Figure 2 were derived for every 10° in longitude and then fit with the same hyperbolic tangent multiplied by a sine function

$$\mathrm{CentEq2}\left(R,\mathrm{Elon}\right) = \left[a\tan h\left(b\times R - c\right) + d\right]\times \sin\left(\mathrm{Elon} - e\right) \tag{2}$$

The mean squared error (MSE) of Equation 2 is 0.0044, where a mean squared error closest to zero is useful for predictions. A fit function 1 percent larger than Equation 2 has an MSE of 0.015. A fit function 1% smaller than Equation 2 has an MSE of 0.0057. These parameters were found using MatLab's goodness of fit function with the MSE cost function.

Table 1
Constants for Equations 1 and 2

a	b	c	d	e
1.66°	0.131	1.62	7.76°	249°

Given the simplicity of the input dipole and washer-shaped current sheet, perhaps it is not surprising that this simple function worked well. Figure 3 shows curves for sample longitudes using Equation 2. Inside ~5 R_J, the dipole $\theta_c = 2/3\ \theta_m$ is a reasonable approximation while beyond ~20–25 R_J $\theta_c = \theta_m$. Figure 4 illustrates the resulting geometry for the meridian plane for the longitudes of maximum tilt of the system. The blue line shows the subtle deviation of the resulting centrifugal equator from a straight line.

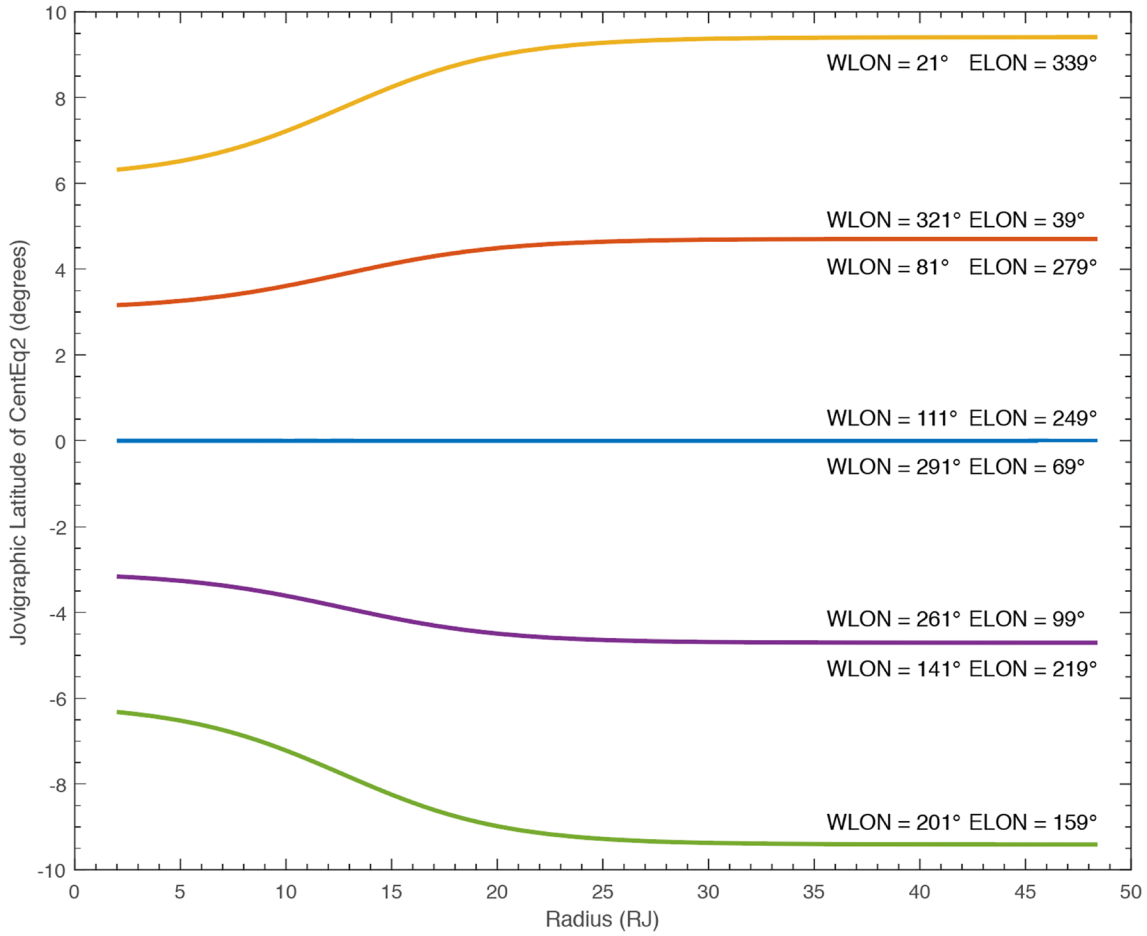

Figure 3. Jovicentric latitude versus Radial distance using the CentEq2 of Equation 2 for selected longitudes.

4. Future Work

The next step is to test this simple functional form for the centrifugal equator against Juno observations of the thermal plasma in Jupiter's magnetosphere (Bagenal et al., 2017). Juno's JADE instrument (McComas et al., 2017) has been observing plasma properties primarily in the outer magnetosphere and over Jupiter's poles (e.g., Ebert et al., 2017; Kim et al., 2020; Szalay et al., 2017; Valek et al., 2019). Radio occultations using

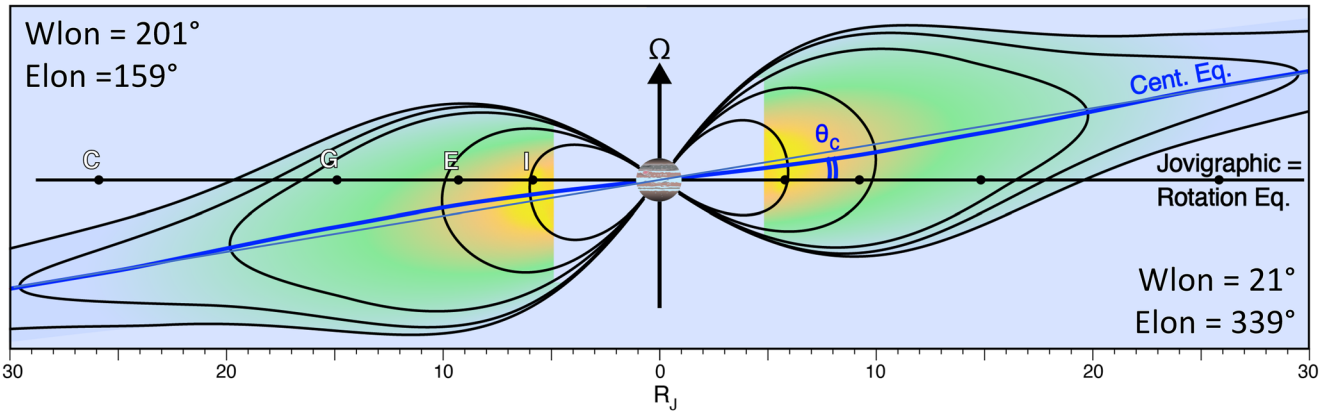

Figure 4. Magnetic field lines, the centrifugal equator (CentEq2), and sketch of the corresponding distribution of plasma density for the longitudes of maximum tilt.

the Juno gravity signals have been used to determine plasma properties in the Io plasma torus ($R = 5$–$10\ R_J$) (Phipps et al., 2018, 2019). Phipps et al. (2020) compared the geometry of the radio occultations (where the path of Juno's radio communication with Earth is modulated by the electron density as it passes through the Io plasma torus) to a modeled centrifugal equator and found similarities in longitude variability in torus densities. The radio occultation measurements could be used to compare with our simple functional form (Equation 2) for the centrifugal equator in the Io plasma torus region of Jupiter's magnetosphere.

Latitudinal precession of Juno's orbit due to Jupiter's oblateness is bringing the inbound equatorial crossing closer to Jupiter so that plasma measurements transecting the plasma sheet could be compared with our formulation for CentEq2. Not only will average location of the center of the plasma disk test the appropriateness of the physical quantities describing VIP4dipole + CON2020 (and corresponding fit parameters in Equation 2 for CentEq2) but coverage over the next ~5 years may reveal temporal variabilities in such properties of the current sheet.

Further studies of Juno magnetic field data may indicate the need for a more complex current sheet in the middle to outer magnetosphere, along the lines of the Khurana model, as applied to Galileo data by Vogt et al. (2015, 2017), as started with Juno data by Connerney et al. (2020) and derived by combining Galileo and Juno data by Lorch et al. (2020). The plasma in the outer magnetosphere is sufficiently hot that it is not very sensitive to changes in the field geometry. In the inner magnetosphere, however, the location of cold plasma in the thin torus inside Io's orbit is very sensitive to the field geometry and it will be important to include the higher-order, nondipole components of the internal field to match plasma data that may be obtained should Juno be extended beyond the prime mission.

5. Summary

To summarize this short note, we have derived a new, simple formulation for the centrifugal equator—farthest point along a magnetic flux tube from Jupiter's spin axis—for the inner magnetosphere (~5–30 R_J), in the following way:

- We have taken a simple dipole magnetic field (tilted 9.5° toward System III longitude of Wlon = 201°) and a washer-shaped disk current sheet (based on Connerney et al., 1981, 2020) to derive a simple model (VIP4dipole + CON2020)
- We find the centrifugal equator along fluxtube for a specific longitude and fit a hyperbolic tangent function to the model locations
- The latitudinal angle of the derived centrifugal equator relative to the jovigraphic equator changes from the dipolar value (2/3 of the dipole tilt) around 5 R_J to close to the full dipole tilt at 25 R_J. This is the key region for the plasma environment between Io and the other Galilean satellites (Bagenal & Dols, 2020)
- We find a good match to the magnetic field model locations by varying the centrifugal equator formula sinusoidally with longitude
- This simple model is only applicable for the equatorial region ~5–30 R_J. Inside ~5 R_J the nondipole components of the magnetic field become important. Outside ~30 R_J the current sheet loses azimuthal symmetry

For the future, we plan to apply our simple centrifugal equator formula (CentEq2) to compare with plasma data (Voyager, Galileo, Juno) obtained on crossings of the plasma sheet, and to from the spacecraft to the equator as well as integrating along the field line to obtain total fluxtube content.

Data Availability Statement

No data are used in this study.

Acknowledgments
We thank Marissa Vogt for assistance with magnetic field code. The work by FB at the University of Colorado was supported as a part NASA's Juno mission supported by NASA through contract 699050X with the Southwest Research Institute. The work by PP was supported in part by NASA Award 80NSSC19K0818.

References

Bagenal, F. (1994). Empirical model of the Io plasma torus: Voyager measurements. *Journal of Geophysical Research*, *99*, 11043–11062.
Bagenal, F., Adriani, A., Allegrini, F., Bolton, S. J., Bonfond, B., Bunce, E. J., et al. (2017). Magnetospheric science objectives of the Juno mission. *Space Science Reviews*, *213*, 219–287. https://doi.org/10.1007/s11214-014-0036-8

Bagenal, F., & Dols, V. (2020). The space environment of Io and Europa. *Journal of Geophysical Research: Space Physics*, *125*, e2019JA027485. https://doi.org/10.1029/2019JA027485

Connerney, J. E. P., Acuña, M. H., & Ness, N. F. (1981). Modeling the Jovian current sheet and inner magnetosphere. *Journal of Geophysical Research*, *86*, 8370–8384. https://doi.org/10.1029/JA086iA10p08370

Connerney, J. E. P., Acuna, M. H., Ness, N. F., & Satoh, T. (1998). New models of Jupiter's magnetic field constrained by the Io flux tube footprint. *Journal of Geophysical Research*, *103*, 11929–11940.

Connerney, J. E. P., Kotsiaros, S., Oliversen, R. J., Espley, J. R., Joergensen, J. L., Joergensen, P. S., et al. (2018). A new model of Jupiter's magnetic field from Juno's first nine orbits. *Geophysical Research Letters*, *45*, 2590–2596. https://doi.org/10.1002/2018GL077312

Connerney, J. E. P., Timmins, S., Herceg, M., & Joergensen, J. L. (2020). A jovian magnetodisc model for the Juno era. *Journal of Geophysical Research: Space Physics*, *125*. https://doi.org/10.1029/2020JA028138

Ebert, R. W., Allegrini, F., Bagenal, F., Bolton, S. J., Connerney, J. E. P., Clark, G., et al. (2017). Spatial distribution and properties of 0.1–100 keV electrons in Jupiter's polar auroral region. *Geophysical Research Letters*, *44*, 9199–9207. https://doi.org/10.1002/2017GL075106

Gledhill, J. A. (1967). Magnetosphere of Jupiter. *Nature*, *214*, 155–156.

Herbert, F., Schneider, N. M., & Dessler, A. J. (2008). New description of Io's cold plasma torus. *Journal of Geophysical Research*, *113*, A01208. https://doi.org/10.1029/2007JA012555

Hess, S. L. G., Bonfond, B., Zarka, P., & Grodent, D. (2011). Model of the Jovian magnetic field topology constrained by the Io auroral emissions. *Journal of Geophysical Research*, *116*, A05217. https://doi.org/10.1029/2010JA016262

Hill, T. H., Dessler, A. J., & Michel, F. C. (1974). Configuration of the jovian magnetosphere. *Geophysical Research Letters*, *1*, 3.

Hill, T. H., & Michel, F. C. (1976). Heavy ions from the Galilean satellites and the centrifugal distortion of the jovian magnetosphere. *Journal of Geophysical Research*, *81*, 4561–4565.

Khurana, K. K. (1997). Euler potential models of Jupiter's magnetospheric field. *Journal of Geophysical Research*, *102*, 11295–11306.

Khurana, K. K., & Schwarzl, H. K. (2005). Global structure of Jupiter's magnetospheric current sheet. *Journal of Geophysical Research*, *110*, 7227. https://doi.org/10.1029/2004JA010757

Kim, T. K.-H., Ebert, R. W., Valek, P. W., Allegrini, F., McComas, D. J., Bagenal, F., et al. (2020). Survey of ion properties in Jupiter's plasma sheet: Juno JADE-I observations. *Journal of Geophysical Research: Space Physics*, *125*, e2019JA027696. https://doi.org/10.1029/2019JA027696

Lorch, C. T. S., Ray, L. C., Arridge, C. S., Khurana, K. K., Martin, C. J., & Bader, A. (2020). Local time asymmetries in Jupiter's magnetodisc currents. *Journal of Geophysical Research: Space Physics*, *125*, e2019JA027455. https://doi.org/10.1029/2019JA027455

McComas, D. J., Alexander, N., Allegrini, F., Bagenal, F., Beebe, C., Clark, G., et al. (2017). The jovian auroral distributions experiment (JADE) on the Juno mission to Jupiter. *Space Science Reviews*, *213*, 547–643. https://doi.org/10.1007/s11214-013-9990-9

Mei, Y., Thorne, R. M., & Bagenal, F. (1995). Analytical model for the density distribution in the Io plasma torus. *Journal of Geophysical Research*, *100*, 1823–1828.

Meyer-Vernet, N. (2001). Large-scale structure of planetary environments: The importance of not being Maxwellian. *Planetary and Space Science*, *49*, 247–260.

Moncuquet, M., Bagenal, F., & Meyer-Vernet, N. (2002). Latitudinal structure of outer Io plasma torus. *Journal of Geophysical Research*, *107*(A9), 1260. https://doi.org/10.1029/2001JA900124,2002

Phipps, P. H., Withers, P., Buccino, D. R., Yang, Y. M., Parisi, M., et al. (2020). Where is the Io plasma torus? A comparison of observations by Juno radio occultations to predictions from Jovian Magnetic field models. *Journal of Geophysical Research: Space Physics*, *125*. https://doi.org/10.1029/2019JA027633

Phipps, P. H., Withers, P., Buccino, D. R., & Yang, Y.-M. (2018). Distribution of plasma in the Io plasma torus during Juno Perijove 1. *Journal of Geophysical Research: Space Physics*, *123*, 6207–6222. https://doi.org/10.1029/2017JA025113

Phipps, P. H., Withers, P., Buccino, D. R., Yang, Y.-M., & Parisi, M. (2019). Variations in the density distribution of the Io plasma torus as seen by radio occultations on Juno Perijoves 3, 6, and 8. *Journal of Geophysical Research: Space Physics*, *124*, 5200–5221. https://doi.org/10.1029/2018JA026297

Siscoe, G. L. (1977). Equatorial confinement and velocity space distribution of satellite ions in Jupiter's magnetosphere. *Journal of Geophysical Research*, *82*, 1641–1645.

Szalay, J. R., Allegrini, F., Bagenal, F., Bolton, S., Clark, G., Connerney, J. E. P., et al. (2017). Plasma measurements in the Jovian polar region with Juno/JADE. *Geophysical Research Letters*, *44*, 7122–7130. https://doi.org/10.1002/2017GL072837

Thomas, N., Bagenal, F., Hill, T. W., & Wilson, J. K. (2004). The Io neutral clouds and plasma torus. In F. Bagenal, T. E. Dowling & W. B. McKinnon (Eds.), *Jupiter: The planet, satellites, and magnetosphere* (pp. 561–592). New York, NY: Cambridge University Press.

Valek, P. W., Allegrini, F., Bagenal, F., Bolton, S. J., Connerney, J. E. P., Ebert, R. W., et al. (2019). Jovian high-latitude ionospheric ions: Juno in situ observations. *Geophysical Research Letters*, *46*, 8663–8670. https://doi.org/10.1029/2019GL084146

Vogt, M. F., Bunce, E. J., Kivelson, M. G., Khurana, K. K., Walker, R. J., Radioti, A., et al. (2015). Magnetosphere-ionosphere mapping at Jupiter: Quantifying the effects of using different internal field models. *Journal of Geophysical Research: Space Physics*, *120*, 2584–2599. https://doi.org/10.1002/2014JA020729

Vogt, M. F., Bunce, E. J., Nichols, J. D., Clarke, J. T., & Kurth, W. S. (2017). Long-term variability of Jupiter's magnetodisk and implications for the aurora. *Journal of Geophysical Research: Space Physics*, *122*, 12090–12110. https://doi.org/10.1002/2017JA024066